Adsorption of C_{60} on nickel clusters at high temperature

E. K. Parks, K. P. Kerns, and S. J. Riley
Chemistry Division, Argonne National Laboratory, Argonne, Illinois 60439

B. J. Winter
Max-Born-Institut für Nichtlineare Optik und Kurzzeitspektroskopie, Rudower Chaussee 6, D-12489 Berlin, Germany
(Received 5 October 1998)

The adsorption of C_{60} on nickel clusters has been studied in a flow-tube reactor at temperatures between 823 and 1073 K. Saturation coverages of C_{60} have been determined for Ni_2–Ni_{72} and show a size dependence consistent with C_{60} adsorption on essentially spherical Ni_n clusters. There is no evidence for C_{60} decomposition. The configuration of the adsorbed C_{60} molecules appears to change from tetrahedral→octahedral→cubic→less symmetrical arrangements as metal cluster size increases. An RRK modeling of the first C_{60} that binds to the nickel clusters yields a binding energy in excess of 2.06 eV. The binding energy appears to decrease with decreasing metal nuclearity of the binding site, with binding to atop sites on the Ni_n clusters being relatively weak. It is argued that electron transfer to the C_{60} ligands is limited by charging of the central Ni_n core and that this may provide a way of controlling the extent of electron transfer to the adsorbed molecules. [S0163-1829(99)03720-0]

I. INTRODUCTION

The interaction of C_{60} with metals has been the subject of many investigations. C_{60} has been adsorbed on metal surfaces[1] and metals have been adsorbed on individual C_{60} molecules,[2] as well as on surfaces of solid C_{60}.[3,4] These wide ranging studies have been possible, in part, because of the incredible stability of the C_{60} molecule. Isolated in the gas phase at 1273 K, C_{60} has a 15-min lifetime for decomposition.[5] At higher temperatures, decomposition with loss of C_2 (Refs. 6–8) or even thermal ionization occurs.[9,10] When metals are adsorbed on individual C_{60} molecules, it is found that in some cases the entire molecule can be coated with metal[2] while in other cases metal adsorption leads to destruction of the C_{60} cage.[11] At higher temperatures, insertion of metal atoms (including Ni) into the C_{60} lattice is observed.[12]

The adsorption of C_{60} on metal surfaces shows a wide variety of behaviors. While the C_{60}-surface interaction was once believed to be van der Waals, most recent studies find it to have both covalent and polar character, and the binding is often strong enough to cause adsorbate-induced surface reconstruction.[1] Charge transfer from metals to C_{60} molecules varies from negligible for C_{60} adsorbed on Pt (111) (Ref. 13) to more than six electrons for K_nC_{60} compounds,[14] showing the incredible versatility of the C_{60} molecule to adapt itself to specific environments. There is interest in finding methods to control the charge transfer as a means of altering the electronic properties of the C_{60}. As we will argue below, adsorbing C_{60} on metal clusters may be one way of providing that control.

There have been a few studies of the interaction of C_{60} with metal clusters. Clustering of C_{60} around Au clusters has been reported in the deposition of Au on a film of C_{60}.[3] Recent studies of the adsorption of C_{60} molecules on small clusters of V,[15,16] Co,[17] Sc,[16] Ti,[16] and Cr,[16] have been reported using a pulsed laser vaporization technique for generating both the metal clusters and C_{60}. Clusters containing up to five metal atoms were studied in most cases. In these experiments a vaporized plume of metal in a helium carrier gas was passed through a vaporized plume of C_{60}, followed by rapid cooling to room temperature. An unknown aspect of these experiments (or at least one not discussed by the authors) is the degree to which the observed $M_n(C_{60})_m$ species are a consequence of kinetics-dominated metal-C_{60} collisions in the gas stream (including C_{60} condensation) rather than equilibrium adsorption that reflects the energetics of C_{60}-metal bonding. Clear differences in the product species for different metals suggest that some sampling of the bonding energetics was being made.

In the present study we examine the adsorption of C_{60} molecules on nickel clusters from Ni_2 through Ni_{72} isolated in the gas phase. In contrast to the earlier cluster studies, the adsorption is studied in a flow-tube reactor (FTR) at high temperature. A controlled temperature environment permits us to more readily distinguish adsorption dominated by kinetics processes from equilibrium C_{60} adsorption. Our observation of equilibrium C_{60} adsorption/desorption is, as far as we are aware, the first demonstration that C_{60} can be desorbed from a nickel surface intact. Previous attempts to desorb C_{60} by laser heating have resulted in metal desorption or C_{60} decomposition instead.[18] These results suggest a lower rate of decomposition on nickel clusters than on bulk nickel surfaces. The probable origin of this difference will be discussed below.

In Sec. II we give experimental details regarding the high-temperature flow-tube reactor and the operating conditions for cluster formation and C_{60} addition to the nickel clusters. In Sec. III we give the experimental results for adsorption of C_{60} on both pure Ni_n clusters and the cluster oxides Ni_nO, and in Sec. IV we discuss what these experiments are telling us about the nature of the $Ni_n(C_{60})_m$ and $Ni_nO(C_{60})_m$ species.

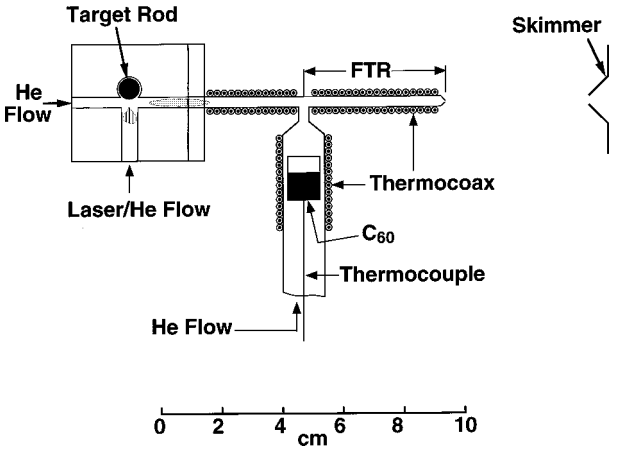

FIG. 1. Schematic of the high-temperature cluster source/flow-tube reactor.

II. EXPERIMENT

Nickel clusters are made by laser vaporization of isotopically pure nickel (^{58}Ni or ^{60}Ni) into a stream of helium gas held between 55 and 75 Torr pressure. The nickel target is formed by electroplating nickel onto a 0.560-cm-diam copper rod. The aluminum block housing the target rod and laser entrance port is the same as that used earlier for chemical probe studies.[19] The flow tube and source for C_{60}, fabricated of stainless steel, is a second assembly that attaches to the aluminum block via a stainless steel flange. A schematic of the entire source/flow tube is shown in Fig. 1. The length (10.6 cm) and inner diameter (3 mm) of the flow tube as well as the nozzle aperture (1 mm) are the same as used in previous studies.[20] The flow tube is wrapped with coaxial heating wire and three layers of Ta heat shields. The C_{60} sample is located within a side arm, also heated with coaxial heating wire surrounded by heat shields, attached to the middle of the flow tube. The C_{60} is placed in a cylindrical cup made of graphite, quartz, or stainless steel and heated by radiation from the side arm. The cup is supported by a 0.159-cm-dia encapsulated chromel-alumel thermocouple that also provides an accurate measure of the cup temperature. Helium is passed through the side arm to transport the C_{60} into the flow tube reactor (FTR), the portion of the flow tube that is downstream of the C_{60} entrance port (see Fig. 1). The FTR and C_{60} sample can be independently heated to 1320 K. Temperature differences of up to 500 K can be maintained between the nozzle and cup. Besides the thermocouple supporting the C_{60} cup, thermocouples are placed at the upstream, center, and downstream (nozzle) regions of the flow tube. Unless otherwise stated, the temperatures quoted in this paper refer to the temperatures of the nozzle. The aluminum block housing the target rod can be cooled by passing either water or liquid nitrogen through a brass block attached to the base of the aluminum block. In most experiments the aluminum block was maintained at room temperature. The reaction time for the clusters in the FTR is $\sim$0.4–0.6 ms.

The clusters pass out of the nozzle at the end of the FTR and are collimated by a 3-mm-diam skimmer. The nozzle-skimmer distance is increased from the normal distance of 1.3 to 5 cm to reduce plugging by the C_{60}. After passing through a differential pumping chamber, the clusters pass into a third chamber where they are ionized either by an ArF (6.42-eV photon energy) or F_2 (7.89-eV photon energy) excimer laser and mass analyzed in a reflection time-of-flight (TOF) mass spectrometer with a resolution of $\sim$1000. Multiphoton processes are minimized by keeping the laser fluences low.

Because of the high nozzle temperature and the large size and mass of the C_{60} ligands, the $Ni_n(C_{60})_m$ clusters acquire considerable translational energy in the nozzle expansion.[21] The large ligands result in increased numbers of cluster-He collisions, and thus reduced slippage in the nozzle expansion, producing translational energies higher than would normally be found for other cluster species of comparable mass. Since the axis of the mass spectrometer is perpendicular to the cluster beam, deflection plates within the mass spectrometer redirect motion initially along the cluster beam axis to motion along the mass spectrometer axis. Mass spectra are measured in 20-μs segments, taken with deflection plate settings that direct the appropriate mass range to the detector.

The mass spectra of C_{60} adsorbed on nickel clusters look quite different from those of other molecules adsorbed on the same clusters. In the case of N_2, for example, the entire $Ni_n(N_2)_m^+$ cluster distribution for a given n generally fits on a single 20-μs segment. In contrast, because of the high C_{60} mass, each element of the $Ni_n(C_{60})_m^+$ distribution generally appears in a different 20-μs segment. This makes it difficult to determine accurate values of $\overline{m}$, the average value of m, used in constructing uptake plots ($\overline{m}$ vs $\ln P_{C_{60}}$, where $P_{C_{60}}$ is the C_{60} pressure in the FTR).[22] A more serious limitation, however, is the rather limited range of C_{60} pressures that can be used in these experiments. The limitation is not the temperature achievable in the C_{60} cup, but the combined need for high C_{60} vapor pressure and low cluster temperature in order to achieve a saturated coverage of C_{60} on the clusters. If the vapor pressure of C_{60} transported into the FTR is too high for the FTR temperature, C_{60} condenses on the walls of the FTR and plugs the nozzle.

A necessary, but not sufficient, condition to obtain a saturation coverage of C_{60} on Ni_n is that the adsorption reaction must be in thermodynamic equilibrium (excluding C_{60} condensation, which is not of interest here). The conversion from kinetics-dominated adsorption to equilibrium adsorption occurs when the rate of C_{60} desorption from the clusters within the FTR becomes equal to the time the clusters spend in the FTR.[23] At equilibrium, the rate of desorption equals the rate of adsorption, so we can write the conversion condition as $(\sigma s n v)^{-1} = 0.57$ ms, where σ is the cluster-C_{60} collision cross section, s the sticking probability, n the C_{60} density, v the cluster-C_{60} relative velocity, and 0.57 ms is the approximate time the clusters spend in the FTR at 873 K. Assuming $\sigma = 100$ Å^2 and $s = 1$ at an FTR temperature of 873 K, we obtain a C_{60} pressure of 1.0 mTorr. This agrees well with the observed conversion pressures for most systems studied.[24] The highest C_{60} pressure used in the present experiments was nominally 18 mTorr, or more than an order of magnitude higher than the conversion pressure. The C_{60} pressure was determined from the mass of C_{60} initially placed in the cup, the length of time before it was exhausted, and the measured flow velocity through the FTR.[25] A C_{60} pressure of 18 mTorr permits nozzle temperatures as low as

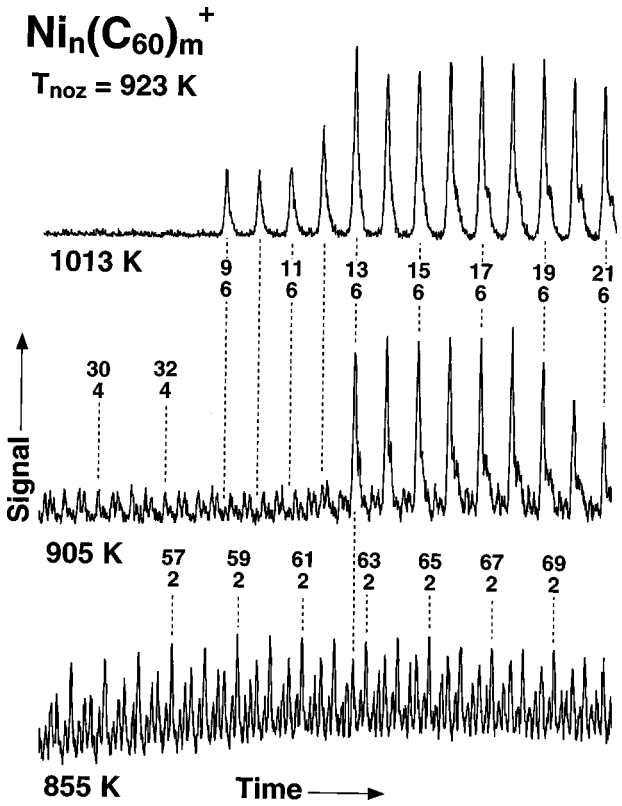

FIG. 2. Mass spectra of $Ni_n(C_{60})_m^+$ at a nozzle temperature of 923 K and three temperatures of the C_{60} cup, 855, 905, and 1013 K, corresponding to increasing C_{60} pressure in the FTR. The three spectra illustrate the conversion from adsorption dominated by kinetics to one dominated by equilibrium processes.

~823 K, below which significant C_{60} condensation occurs in the FTR.

In Fig. 2 we show mass spectra (single 20-μs segments of the entire mass spectrum) at three different temperatures of the C_{60} cup and a nozzle temperature of 923 K. Ionization was with an F_2 laser. At a cup temperature of 855 K (the bottom spectrum), each Ni_n cluster shows a large number of $Ni_n(C_{60})_m^+$ peaks characteristic of adsorption dominated by kinetics. As the cup temperature is increased, the spectra begin to simplify and at 1013 K (the top spectrum), corresponding to nominally 18 mTorr C_{60}, single $Ni_n(C_{60})_m^+$ peaks are seen for most clusters and the adsorption reaction is clearly in equilibrium. Under these conditions all the Ni_n clusters from Ni_9 through Ni_{21} appear to have become saturated at $Ni_n(C_{60})_6$. It must be reiterated that saturation is not guaranteed by the appearance of equilibrium adsorption. Higher pressures are often necessary to adsorb more weakly bound molecules. However, since the accessible C_{60} pressure range is so small with the present experimental configuration, it is not possible to raise the C_{60} pressure to test for further adsorption. The presence or absence of saturation can, in an approximate way, be tested by the temperature dependence of the C_{60} coverage. A coverage that is insensitive to a large change in cluster temperature for the same pressure of C_{60} can be assumed to be saturated.

The assignment of peaks in the mass spectra is complicated by the approximate mass overlap of the $Ni_n(C_{60})_mO^+$ and $Ni_{n+25}(C_{60})_{m-2}^+$ peaks for the ^{58}Ni isotope and the fact

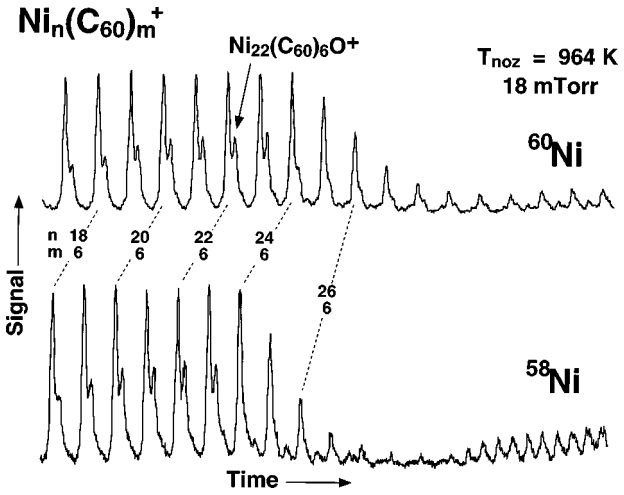

FIG. 3. Mass spectra of $Ni_n(C_{60})_m^+$ for both the ^{58}Ni and ^{60}Ni isotopes, illustrating that the shoulders on the most intense peaks are indeed cluster oxides. The nozzle temperature was 964 K and the C_{60} cup temperature was 1013 K.

that cluster oxides are always present to some extent in the cluster distribution. While these two species are 6 amu apart, apparent mass shifts due to the different numbers of C_{60} molecules adsorbed on the clusters result in an inability to resolve the two peaks in the mass spectra.[26] To help in peak identification, mass spectra were taken with both ^{58}Ni and ^{60}Ni. Since the mass of C_{60} is equal to 12 times the mass of ^{60}Ni (in the absence of ^{13}C), the $Ni_n(C_{60})_m^+$ peaks in the ^{60}Ni spectra form a single series of peaks that is coincident (aside from slight broadening due to the ligand-dependent mass shifts) with the series of bare cluster peaks Ni_n^+. All oxide peaks will fall outside this series of peaks. This is illustrated in Fig. 3, where we show 20-μs segments of the mass spectra for both ^{58}Ni and ^{60}Ni. A comparison of the spectra clearly show that the small peaks on the right shoulder of the larger peaks are indeed cluster oxides and that there is an abrupt change in the C_{60} coverage on the oxide clusters at Ni_{24}.

It is important in studies of cluster reactivity that cluster growth terminates and the clusters thermalize prior to the addition of reagent gas. Otherwise, the clusters may be at high temperature (higher than the temperature of the FTR at the point where reagent gas is added) and decomposition of the cluster-reagent adduct may occur. [In the present experiments decomposition of cluster oxides with an adsorbed layer of C_{60}, $Ni_nO(C_{60})_m$, is observed at nozzle temperatures above 1073 K.[27]] It has been previously determined that at room temperature and 20-Torr He pressure, cluster growth is terminated by the time the clusters reach a point 4 cm downstream of the target rod.[20] Cluster growth terminates because diffusional loss of metal atoms to the wall of the flow tube depletes the atom density sufficiently that no further collisions between the clusters and the residual atoms occur. At temperatures other than room temperature, the ratio of P/T, the pressure in the flow tube divided by the temperature, is kept constant in an attempt to keep the diffusional loss at a constant rate and ensure a termination of cluster growth upstream of the entrance port of the FTR. Increasing the helium pressure above the nominal pressure causes cluster growth to continue past the reagent port and can yield mass spectra

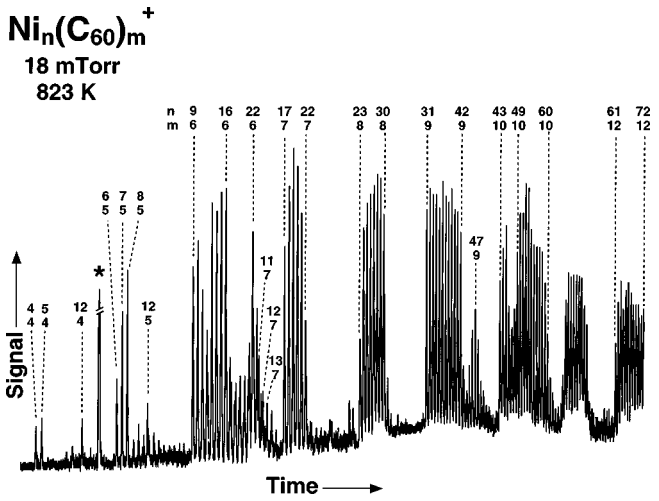

FIG. 4. A composite mass spectra from $Ni_4(C_{60})_4$ through $Ni_{72}(C_{60})_m$ formed from eleven 20-μs segments. The nozzle temperature was 823 K and the nominal C_{60} pressure was 18 mTorr. The peak labeled with an asterisk is an impurity in the C_{60} sample.

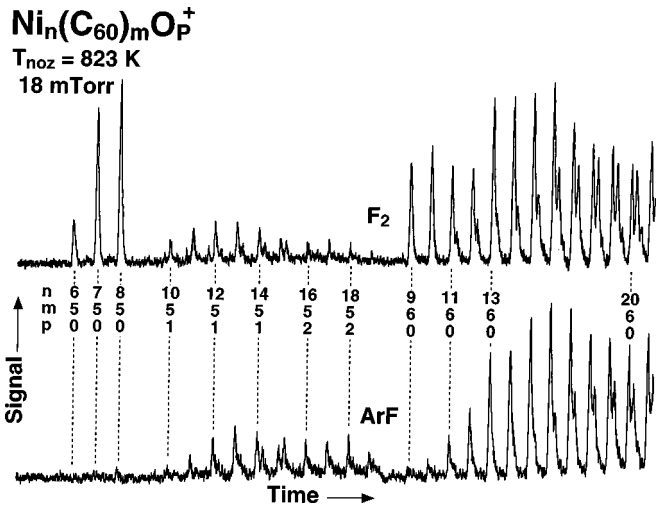

FIG. 5. A comparison of mass spectra for F_2 and ArF laser ionization in the size region corresponding to onset of $Ni_n(C_{60})_m$ ionization with the ArF laser.

with unusual distributions of products or peaks associated with decomposition of the cluster-reagent adduct. In the present experiments no unusual peaks were observed at the nominal temperature and pressure conditions, but a 50% increase in helium pressure in the FTR produced a large number of new peaks corresponding to less completely saturated clusters. It is not known whether these species are the result of decomposition, but their presence is clearly related to cluster growth beyond the C_{60} reagent port. The complete absence of these species at the nominal pressure and temperature conditions is a good indicator that under these operating conditions, cluster growth and thermalization of the clusters to the temperature of the FTR are indeed complete before addition of the C_{60} reagent gas.

Three different cup materials were used in the present study. Most experiments were done with a graphite cup, but quartz and stainless steel cups also yielded the same mass spectra. Two sources of C_{60} were used. One from MER Corporation[28] (99.5+%) and the other from Hoechst AG (Ref. 29) (gold grade). Both samples produced the same mass spectra.

III. RESULTS

In Fig. 4 we show a composite mass spectrum assembled from 20-μs TOF segments recorded with a nozzle temperature of 823 K and a nominal C_{60} pressure in the FTR of 18 mTorr. Actually, a small degree of nozzle plugging was observed at this temperature, suggesting some C_{60} condensation on the walls of the FTR and a C_{60} pressure somewhat lower than 18 mTorr. The spectrum includes clusters ions from $Ni_4(C_{60})_4^+$ through $Ni_{72}(C_{60})_{12}^+$. This spectrum shows the highest degree of C_{60} saturation that we have observed for the $Ni_n + C_{60}$ system.

As can be seen in Fig. 4, the peaks naturally fall into groups associated with a specific number of C_{60} molecules adsorbed on the clusters. Using the notation $a(b\text{-}c)$, where a is the number of C_{60} molecules on the cluster and $b\text{-}c$ is the range of nickel clusters that adsorb ''a'' C_{60} molecules, the groupings for significant peaks in Fig. 4 are 4(4–5), 5(6–8), 6(9–16) and 6(22–23), 7(17–22), 8(23–30), 9(31–42) and 9(46–48), 10(43–60), and 12(61–72). The group of peaks in Fig. 4 between $Ni_{60}(C_{60})_{10}$ and $Ni_{61}(C_{60})_{12}$ includes some clusters with 11 adsorbed C_{60} molecules, but most of the signal in this region corresponds to $Ni_nO(C_{60})_{11}$ species. Spectra similar to that shown in Fig. 4, but differing in the coverage level for some clusters, are observed at temperatures up to 1073 K. The peak labeled with an asterisk in Fig. 4 corresponds to an impurity in the C_{60} vapor that appears with every sample of C_{60} we have used and is present when no nickel clusters are being generated. Its intensity is roughly a factor of 1000 lower than that of C_{60}. When the C_{60} sample is depleted, this peak also disappears. Its mass is approximately 3750 and its composition is unknown.[30]

At F_2 laser fluences roughly twice those used in Fig. 4, additional peaks begin to appear in the mass spectra. Some of these peaks can be identified as $Ni_n(C_{60})_m^+$ species that result from multiphoton desorption of C_{60} from the saturated clusters. It is of interest that desorption of C_{60} can actually result from laser heating of nickel clusters, since pulsed laser excitation of C_{60} on Ni(111) to reach surface temperatures as high as 2000–3000 K shows Ni desorption, but no C_{60} desorption.[18]

Mass spectra essentially identical to those in Fig. 4 were obtained with ArF laser ionization for nickel clusters larger than ~13 atoms, although the ionization efficiency was smaller. Unless otherwise stated, the results presented here were recorded with F_2 laser ionization. A mass spectrum in the region of 13 atoms is shown in Fig. 5 for both F_2 and ArF laser ionization. Reducing the ArF laser fluence by a factor of 5 yielded a factor of 5 reduction in ion signal and a mass spectrum identical to the ArF spectrum in Fig. 5, implying one-photon ionization. The lower energy photons of the ArF laser ionize the *saturated* $Ni_n(C_{60})_m$ clusters with $n \geq 10$. For $n < 10$, some cluster oxides, $Ni_nO(C_{60})_m$, were ionized, but no $Ni_n(C_{60})_m$ clusters were ionized other than $Ni_3(C_{60})_2$. Ni_6 is particularly interesting, as its appearance in the mass spectra shows an unusual dependence on C_{60} coverage. Ni_6 has an ionization potential greater than 6.42 eV,[31] and cannot be

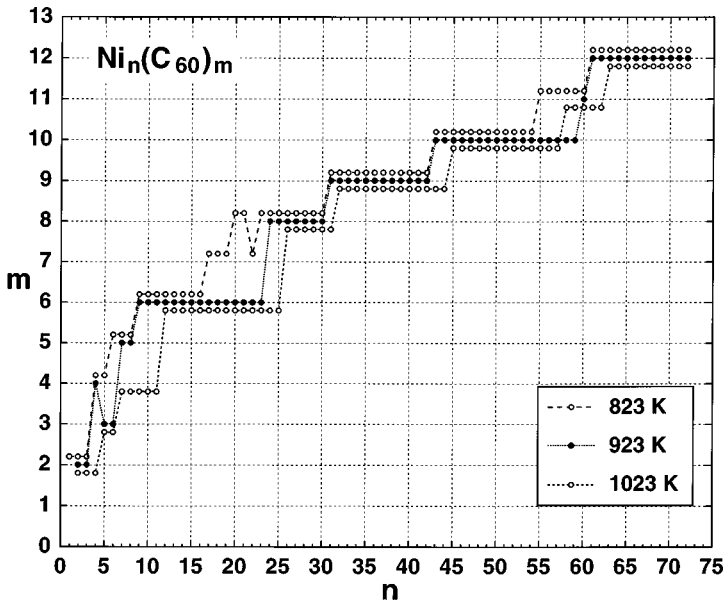

FIG. 6. The coverages of C_{60} observed at three different nozzle temperatures, 823, 923, and 1023 K, with the C_{60} cup at 1013 K.

ionized by the ArF laser. Ni_6C_{60} and $Ni_6(C_{60})_3$ can be ionized, while $Ni_6(C_{60})_2$ and $Ni_6(C_{60})_5$ cannot (although both can be ionized by the F_2 laser). $Ni_6(C_{60})_4$ is not seen with either laser, most likely due to a rapid adsorbate-induced transition from $Ni_6(C_{60})_3$ to $Ni_6(C_{60})_5$. The significance of the unusual ionization behavior of Ni_6 will be discussed in Sec. IV.

In Fig. 6 we present a plot of the highest C_{60} coverages on the nickel clusters vs cluster size at 823, 923, and 1023 K for a fixed cup temperature. An *m* value is included in the figure if the $Ni_n(C_{60})_m^+$ intensity is greater than 10% of the $Ni_n(C_{60})_{m-1}^+$ intensity.

In Fig. 7 we show mass spectra in the lowest mass region. In the lower spectrum, recorded at a cluster temperature of 873 K, peaks corresponding to atomic nickel, the nickel dimer, and the nickel trimer are seen, each binding two C_{60} molecules. At 1073 K (upper spectrum), the atomic nickel peak disappears and a new peak appears corresponding to a pentamer oxide bound to two C_{60} molecules. Small peaks corresponding to $Ni_4(C_{60})_2^+$ and $Ni_4O(C_{60})_2^+$ also are seen. The appearance of the monomer, dimer, and trimer species is somewhat unexpected. With no C_{60} present, the smallest Ni_n^+ cluster that is seen is Ni_5^+. Small clusters diffuse rapidly to the wall of the flow tube at the relatively low helium pressures used in these experiments, and by the end of the FTR there is a negligible density of these species. This does not mean, however, that the corresponding $Ni_n(C_{60})_m$ species would not be observed. When the small Ni_n clusters adsorb C_{60} in the FTR, their size dramatically increases and their diffusional loss decreases. The question then is whether the $Ni_2(C_{60})_2^+$ and $Ni_3(C_{60})_2^+$ ions result from saturation of Ni_2 and Ni_3 or whether they arise from fragmentation processes, either one-photon or two-photon absorption or possibly induced directly by the adsorption of C_{60} on larger clusters. The fluence dependence of the $Ni_2(C_{60})_2^+$ and $Ni_3(C_{60})_2^+$ species is consistent with one-photon adsorption.

In order to resolve this question, the aluminum source block was cooled to 153 K, while the nozzle temperature was held at 873 K and the FTR pressure was the nominal 65 Torr appropriate for this temperature. This has the effect of increasing the helium density in the region of the target rod, thereby decreasing the diffusional loss of metal atoms in the upstream part of the flow tube. Under these conditions and with a cool C_{60} cup, species as small as Ni_2^+ were observed in the mass spectra,[32] suggesting that $Ni_2(C_{60})_m$ and $Ni_3(C_{60})_m$ ions arising from adsorption on the nascent bare Ni_2 and Ni_3 clusters should clearly be seen in the mass spectra. With the cold source block and the C_{60} pressure at 18 mTorr, the $Ni_2(C_{60})_2$ and $Ni_3(C_{60})_2$ species were seen as the only reaction products of these clusters. In fact, these species were observed at an order of magnitude lower C_{60} pressure, where Ni_4 has already saturated at $Ni_4(C_{60})_4$. Thus, we conclude that both Ni_2 and Ni_3 saturate with the adsorption of two C_{60} molecules.[33]

The increase in C_{60} coverage is not always a smooth function of cluster size. This can be seen particularly clearly in Fig. 8, where we show a mass spectrum in the region of $Ni_8(C_{60})_m$ through $Ni_{12}(C_{60})_m$ recorded at a nozzle temperature of 923 K and a nominal C_{60} pressure of 18 mTorr. The spectrum is clearly bimodal for Ni_9–Ni_{12}, showing

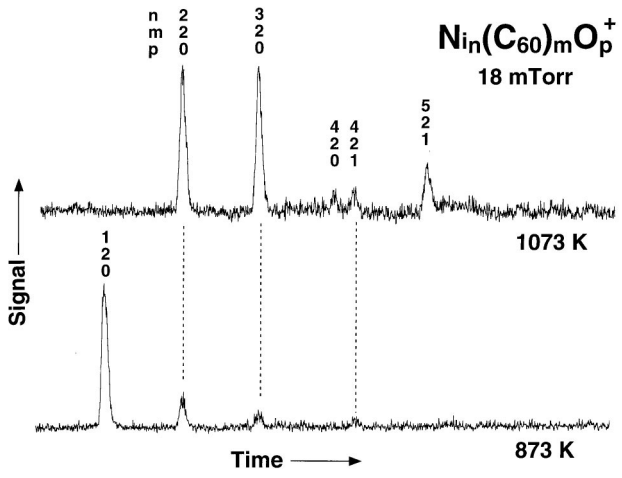

FIG. 7. Mass spectra in the low mass region at nozzle temperatures of 873 and 1073 K and a C_{60} cup temperature of 1013 K.

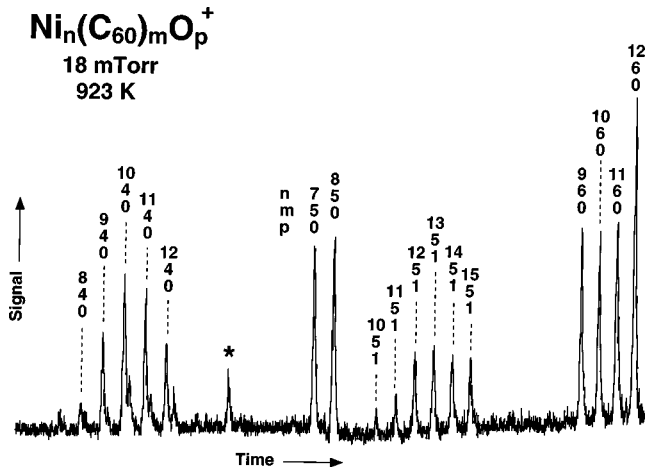

FIG. 8. Mass spectra for $Ni_8(C_{60})_m$ through $Ni_{12}(C_{60})_m$, illustrating the jump in coverage from four to six C_{60} molecules. The peak labeled with an asterisk is an impurity in the C_{60} sample.

$Ni_n(C_{60})_4^+$ and $Ni_n(C_{60})_6^+$ peaks with no intervening $Ni_n(C_{60})_5^+$ peaks. (Most of the peaks between these two groups are cluster oxides.) Similar jumps in coverage are observed at various temperatures for $Ni_{23-27}(6-8)$ and $Ni_{61-64}(10-12)$. Ni_{12} has the most unusual C_{60} pressure dependence of any cluster studied. While there is a clear bimodal distribution at 923 K and 18 mTorr pressure, with only two peaks present in the cluster distribution, at 823 K $Ni_{12}(C_{60})_4^+$, $Ni_{12}(C_{60})_5^+$, $Ni_{12}(C_{60})_6^+$, and $Ni_{12}(C_{60})_7^+$ are all present in the mass spectrum (see Fig. 4).

The jump from $Ni_n(C_{60})_4$ to $Ni_n(C_{60})_6$ that is seen in Fig. 8 implies that some structural change is occurring as a consequence of adsorbing C_{60}. This can occur within the Ni_n cluster itself or in the distribution of C_{60} molecules on the surface of the cluster or both. The occurrence of such a jump is perhaps of even greater interest for Ni_{13}, since Ni_{13} is expected to form as a closed shell, with one atom at the center and 12 atoms outside in one of several possible arrangements. The spectrum analogous to Fig. 8 for Ni_{13} is shown in Fig. 9. In this case, the C_{60} adsorption energies are

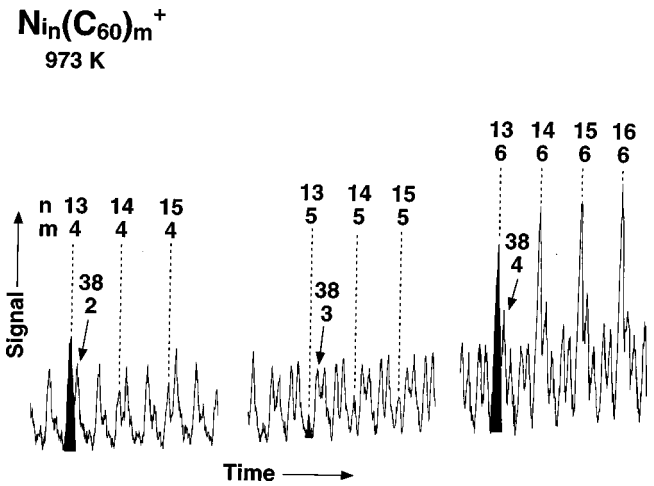

FIG. 9. Mass spectra demonstrating the apparent jump in coverage from $Ni_{13}(C_{60})_4$ to $Ni_{13}(C_{60})_6$. The nozzle temperature was 973 K and the C_{60} cup temperature was 903 K. The $Ni_{13}(C_{60})_m$ peaks are shaded black.

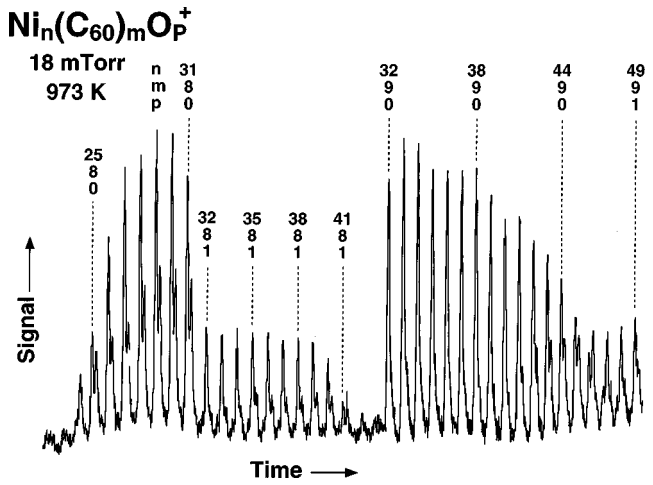

FIG. 10. Mass spectra illustrating the different coverage levels on $Ni_n(C_{60})_m$ and the $Ni_nO(C_{60})_m$ clusters. The nozzle temperature was 973 K and the C_{60} cup temperature was 1013 K.

sufficiently high that equilibrium adsorption is seen only after the adsorption of six C_{60} molecules. The product distribution in Fig. 9 is a reflection of the kinetics of adsorption at a C_{60} pressure just below saturation at $Ni_{13}(C_{60})_6$. The distribution shows significant peaks at $Ni_{13}(C_{60})_4^+$ and $Ni_{13}(C_{60})_6^+$, and a very small peak at $Ni_{13}(C_{60})_5^+$. While a distribution of products in this case can become bimodal without implying a structure change,[34] the smallness of the $Ni_{13}(C_{60})_5^+$ peak suggests that the $4\rightarrow6$ transition observed for Ni_{9-12} is probably also occurring for Ni_{13}. It should be noted that analogous experiments on Co_n clusters show the same series of $Co_n(C_{60})_4\rightarrow Co_n(C_{60})_6$ transitions, and the conversion of $Co_{13}(C_{60})_4\rightarrow Co_{13}(C_{60})_6$ occurs under equilibrium conditions.[35]

Nickel cluster oxides are always present in the cluster distribution to some extent. The C_{60} coverage levels for the $Ni_nO(C_{60})_m$ clusters are not always the same as those for the $Ni_n(C_{60})_m$ clusters. This is illustrated in Fig. 10, where we show a 20-μs segment of the mass spectrum with a nozzle temperature of 973 K and a nominal 18 mTorr C_{60} pressure. From Ni_{24} through Ni_{31}, pure clusters and cluster oxides adsorb eight C_{60} molecules. For Ni_{32}, however, the bare cluster coverage level has abruptly increased by one to $Ni_{32}(C_{60})_9$, while the $Ni_{32}O$ cluster has not changed its C_{60} coverage. (The small peaks on the shoulder of the cluster oxides are cluster dioxides.) This difference continues through approximately Ni_{40} before the ninth C_{60} molecule begins to appear on the oxide cluster. In Fig. 11, we show a comparison of the C_{60} coverage for the bare and oxide clusters at 823 K and a nominal C_{60} pressure of 18 mTorr.

IV. DISCUSSION

A. Saturated clusters

There are a number of questions about the nature of the $Ni_n(C_{60})_m$ species observed in these experiments. Basic questions of geometry include (1) do the nickel clusters that are initially formed upstream of the FTR remain intact in the $Ni_n(C_{60})_m$ species or do the clusters decompose and reform as a matrix of metal and C_{60} similar to the alkali-C_{60} mate-

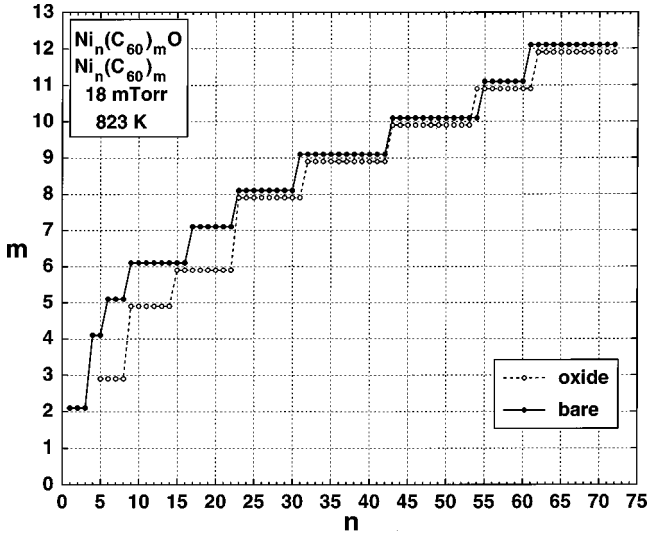

FIG. 11. A comparison of the C_{60} coverage on the nickel and nickel oxide clusters vs cluster size. The nozzle temperature was 823 K and the C_{60} cup temperature was 1013 K.

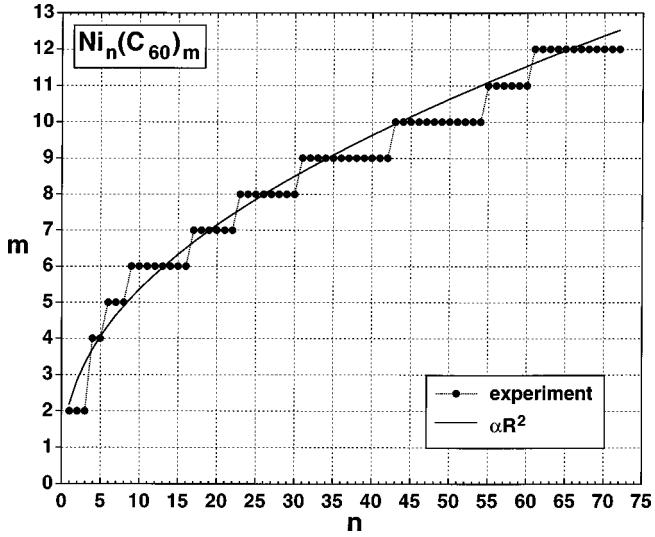

FIG. 12. A comparison of the experimental C_{60} saturation levels and a best-fit plot of αR^2, where R is the distance from the center of the (assumed) spherical nickel cluster to the point of contact between the adsorbed C_{60} molecules and α is an adjustable constant (see the Appendix). The good agreement between the calculated and experimental coverages demonstrates that the C_{60} molecules are adsorbing on essentially spherical Ni_n clusters.

rials discovered earlier;[36] (2) if the nickel clusters are intact, are they liquidlike or solidlike; (3) are the C_{60} molecules intact when adsorbed on the Ni_n clusters or have they decomposed; (4) if the nickel cluster is solidlike and decomposition does not occur, do the C_{60} molecules bind to specific sites on the metal cluster or to the cluster as a whole, and similarly does the metal cluster form bonds to specific sites on the C_{60}, or is the C_{60} molecule free to rotate on the surface of the cluster similar to the partial orientational order observed in the room temperature C_{60} solid;[37] (5) if the Ni_n clusters remain intact following C_{60} adsorption, what happens to their geometrical structure as a consequence of that adsorption; and (6) are saturation coverages obtained at 823 K or can additional molecules adsorb at higher C_{60} pressures? There are additional questions regarding the electronic character of these species. Assuming the Ni_n is intact, (1) what is the degree of charge transfer from Ni_n to C_{60} as a function of C_{60} coverage, (2) does ionization cause removal of an electron from the metal cluster or from C_{60}, and (3) what are the bond strengths of C_{60} to the nickel clusters as a function of coverage? Some of these questions can be answered from the present experimental results, while some will require additional studies.

In Fig. 12 we show the $Ni_n(C_{60})_m$ saturation levels observed at 823 K and a plot of αR^2 vs cluster size, where α is an arbitrary constant and R is the distance from the center of the Ni_n cluster to the point of contact between C_{60} molecules adsorbed on the cluster's surface (see the Appendix). $4\pi R^2$ is an effective area associated with packing C_{60} on the surface. The metal cluster radius is determined from the structureless packing model[38] and the C_{60} radius is taken as 5.0 Å, half the molecular spacing in bulk C_{60}.[39] The curve αR^2 follows closely the observed level of C_{60} adsorption, demonstrating that adsorption is indeed occurring on essentially spherical nickel clusters.

We next consider the issue of C_{60} decomposition. As mentioned earlier, C_{60} in the bulk phase only decomposes at temperatures of 1270 K or above, demonstrating its inherent stability. In contrast, decomposition on the Ni(110) surface has been observed at temperatures as low as 760 K,[13] clearly indicating a catalytic effect of the metal surface on the decomposition rate. On Ni(111) it has been reported[18] that the thermal decomposition lifetime is about 60 s at a surface temperature of 850 K or only 27 K above our lowest temperature. These results demonstrate that C_{60} decomposition depends on the crystal face and thus decomposition on nickel clusters may occur at quite a different rate.

There are several arguments against decomposition occurring on the nickel clusters, at least at the low end (823 K) of the temperature range studied here. While C_{60} decomposes at these temperatures on a Ni(110) surface, the time scale of the present experiments ($\sim$0.5 ms) is 10^{-4}–10^{-3} times that of the surface studies, making decomposition less likely. With a 10^{13} preexponential factor for the rate of a unimolecular decomposition process, a 100-s time constant for decomposition at 760 K would yield a 7-s time constant at 823 K and a 4-ms time constant at 1073 K, still well above the 0.5-ms time scale of the cluster experiments. In addition, as will be discussed below, the cluster-C_{60} interaction is likely weaker than that on the Ni surface, especially under saturated conditions, further reducing the probability for decomposition. Thus, decomposition is unlikely at 823 K and may not be occurring over the entire 823–1073 K range of temperatures studied here. This is consistent with the observation of multiphoton desorption of C_{60} at high fluences of the F_2 laser, which implies that undecomposed molecules are on the clusters' surfaces. The decrease in coverage at 1073 K at the nominal C_{60} pressures of 18 mTorr for essentially all clusters also implies the equilibrium adsorption and desorption of C_{60} molecules from the cluster surfaces, without decomposition.

An attempt was made to desorb a single C_{60} molecule adsorbed on Ni_n by adjusting the C_{60} pressure to produce a low level of coverage, which included Ni_nC_{60} and the bare Ni_n clusters, and then heating the FTR to desorb the C_{60}. [As

mentioned above, attempts to desorb C_{60} from Ni(111) by laser heating were unsuccessful.[18]] No significant change in the $Ni_nC_{60}^+/Ni_n^+$ ratio was observed with increasing temperature up to 1073 K, indicating no desorption of C_{60}. This suggests that either the C_{60}-Ni_n bond strength is quite strong, or decomposition had indeed occurred and the products of decomposition also do not desorb. If decomposition does not occur, then the fact that the desorption lifetime is greater than 0.5 ms (the time the clusters spend in the FTR at 1073 K) can be used to estimate a rough lower bound to E, the C_{60}-Ni_n bond strength. Using the traditional $1\times10^{13}\,s^{-1}$ frequency factor[40] in an RRK analysis, the bond strength can be obtained from the relation $(0.5\times10^{-3})^{-1}=1\times10^{13}\exp(-E/kT)$. This gives 2.06 eV for the C_{60}-Ni_n bond strength, implying a rather strong interaction with the cluster. The frequency factor of 1×10^{13} is, however, somewhat arbitrary, and thus it is difficult to assign an error limit to this value.

There are other indications of strong C_{60} adsorption on bulk nickel surfaces. Valence photoelectron spectra of C_{60} on Ni(110) show substantial broadening of the C_{60} valence bands that are consistent with a strong interaction.[41] The observation of significant electron transfer from the Ni(110) surface to adsorbed C_{60} (Ref. 42) and the above-mentioned decomposition of C_{60} on Ni(110) at relatively low temperature are also indicative of a strong interaction. In spite of the strong interaction, equilibrium adsorption/desorption of C_{60} on nickel clusters can be observed, at least at high temperature and at the higher coverage levels, suggesting that thermodynamic measurements of C_{60} adsorption, analogous to measurements of N_2 adsorption on nickel clusters,[43] may be possible and could provide an accurate measure of the C_{60} adsorption energy.

While the melting point of bulk nickel is 1726 K, metal clusters often melt at considerably lower temperatures.[44] If the nickel clusters in $Ni_n(C_{60})_m$ were actually liquidlike, a continuous increase in m with increasing cluster size, without jumps in the coverage level by more than one molecule, should be expected. Instead there are frequent jumps in coverage by two C_{60} molecules (see, for example, Fig. 8) that are only consistent with solidlike nickel clusters that bind C_{60} molecules to specific sites on the clusters' surfaces. The jumps in coverage can, in principle, result from changes in the nickel cluster structure or changes in the distribution of C_{60} ligands on the surface of the cluster. In either case, an energy barrier to the transition can lead to bimodal distributions of product species, as is observed experimentally. An energy barrier, however, is not required to yield a bimodal distribution. Consider, for example, four C_{60} molecules adsorbed on sites of type ''*a*'' converting to six molecules adsorbed on sites of type ''*b*,'' which have a smaller adsorption free energy. If the free energies are such that $Ni_n(C_{60})_6$ (''*b*'') is more stable than $Ni_n(C_{60})_4$ (''*a*''), but $Ni_n(C_{60})_5$ (''*b*'') is less stable than $Ni_n(C_{60})_4$ (''*a*''), then the observed transition will be from $Ni_n(C_{60})_4^+$ to $Ni_n(C_{60})_6^+$ with very little $Ni_n(C_{60})_5^+$ appearing in the mass spectra.

Changes in the metal cluster structure have been used to explain bimodal distributions seen with nitrogen[22,45] and ammonia[46] adsorption on small nickel clusters. In the present case, however, the observed bimodal distributions are more likely a reflection of changes in the configuration of the C_{60} molecules (possibly coupled with changes in the Ni_n cluster structure). It is difficult, for example, to explain a discontinuous change in coverage by two molecules occurring over a range of sizes (e.g., from Ni_{9-13} or Ni_{23-27}) as arising from a structural change in the bare clusters, as this would require a cluster size *independent* barrier to transformation. A reorganization of the ligands, however, might be expected to persist over a range of cluster sizes if it is due, for example, to the overall size of the Ni_n core. The sequence of coverage levels at $4\rightarrow6\rightarrow8$ observed at some temperatures suggests a sequence tetrahedral→octahedral→cubic arrangements of the C_{60} molecules (see Sec. IV C for specific examples). The fact that these same jumps in coverage are also observed for cobalt clusters[35] is further evidence that they reflect reorganization of the C_{60} ligands.

We can only speculate on the general question of C_{60} mobility based on surface studies. Low-energy electron diffraction measurements[42] on Ni(110) at temperatures between 630 and 660 K show density fluctuations over the surface that are attributed to a relative lack of mobility in comparison to other metal surfaces, yet another indicator of a strong C_{60}-Ni bond. While our temperatures are somewhat higher, the curvature of the clusters' surfaces would be expected to inhibit C_{60} mobility, and this coupled with the observed jumps in coverage suggests that the C_{60} molecules are probably not very mobile, at least on the ms time scale.

The issue of the orientation of the C_{60} molecules on the nickel clusters is not addressed in an obvious way in the present experiments. Recent x-ray photoelectron diffraction studies[47] have shown that on copper and aluminum surfaces, C_{60} adsorbs in a fixed orientation at room temperature. Several configurations were reported, including one with a sixfold face of C_{60} directed toward the surface, one with an edge bond between a sixfold and fivefold face toward the surface, and one with a single atom toward the surface, although the molecule-surface registry was not known. Binding of the fivefold face of C_{60} to an atop site has also been observed on Ag(111) and Au(111).[48] In view of these results, it is likely that C_{60} may have a number of bonding configurations with the nickel clusters. However, due to the higher temperatures in our experiments, the assumption of a fixed orientation of the C_{60} molecule on the surface may not be valid.

We consider finally the question of electron transfer to the adsorbed C_{60} molecules. In general, electron transfer appears to vary considerably on metal surfaces. Platinum, for example, has a negligible degree of electron transfer,[13] although the interaction of C_{60} with the surface is quite strong, indicating considerable covalent bonding. In contrast, on K surfaces,[49] significantly more than six electrons are transferred to each C_{60} molecule. For Ni(110), measurements of the shift in the infrared-active vibrational modes of C_{60} (and their correlation with the C_{60} charge state) have demonstrated a more intermediate level of electron transfer from the metal to C_{60} of 2 ± 1 electrons per C_{60} molecule.[42]

The direction of electron transfer on Ni(110) is in agreement with several observations regarding ionization of the $Ni_n(C_{60})_m$ clusters. A transfer of electrons from a metal cluster to an adsorbed molecule generally results in a decreased ionization efficiency and an increase in the cluster ionization

potential.[50] In the case of $Ni_n(C_{60})_m$, both of these effects are observed. With F_2 laser ionization the measured ionization efficiency of $Ni_n(C_{60})_m$ is roughly a factor of 2 lower than that of the bare cluster, in spite of the fact that the photon energy is above the C_{60} ionization potential (IP), and the IP's of the saturated clusters are clearly higher than those of the bare clusters [with the ArF laser, Ni_5 and Ni_n: $n \geq 7$ can be one-photon ionized; for the clusters saturated with C_{60}, ionization only occurs for $Ni_n(C_{60})_m$: $n \geq 10$ (see Fig. 5)].

Since both the rates of decomposition[43,44] and the binding geometries[47] of C_{60} can be different on different faces of a solid metal surface, the degree of electron transfer from the nickel clusters to C_{60} may vary considerably from cluster to cluster (where structure changes are frequent) and even as a function of C_{60} coverage, because the strong cluster-C_{60} bond may induce structural changes. In addition to these effects, there should be a general decrease of charge transfer with decreasing cluster size due to charging of the Ni_n core. On a metal surface the metal acts as an infinite source of electrons. Thus, every C_{60} molecule adsorbed on a bulk Ni surface may receive two electrons from the metal. A small nickel cluster, however, may not be able to transfer more than a few electrons total to all the adsorbed molecules before the localized charging prevents further electron transfer. Thus, a nickel cluster saturated with C_{60} might have considerably smaller electron transfer per C_{60} molecule than does the bulk surface. This would be expected to result in weaker C_{60} binding to the nickel clusters as compared to nickel surfaces, and a decreased rate of decomposition. This effect will obviously increase with decreasing cluster size.

This charging of the central Ni_n cluster provides a unique way of controlling the electron transfer to the adsorbed molecules. If the $Ni_n(C_{60})_m$ species are sufficiently stable, we can envision preparing monodispersed samples of $Ni_n(C_{60})_m$, where the specific size of the Ni_n cluster correlates with a specific degree of electron transfer to the adsorbed C_{60}. Small clusters would have relatively little electron transfer (due to charging of the Ni_n core), and as cluster size increases, the electron transfer would approach the bulk value of roughly two electrons per C_{60} molecule. Thus, by varying the cluster size, we could vary the optical and electronic properties of the adsorbed C_{60}. By using other metals and alloys it may be possible to expand the range of electron transfer even further.

The Ni_n charging due to C_{60} adsorption can have a substantial effect on the coverage dependence of the electron transfer. If a single C_{60} molecule is adsorbed on a Ni_n cluster, electron transfer will probably be at a maximum, since the bare Ni_n cluster is electrically neutral. If the electron transfer is sufficient, ionization of the resultant species $Ni_n^{\delta+}(C_{60})^{\delta-}$ may occur preferentially from the negatively charged C_{60} molecule and the IP of the $Ni_n^{\delta+}(C_{60})^{\delta-}$ species may be lower than that of the neutral Ni_n cluster. Increasing the coverage (assuming the same underlying Ni_n structure) will result in a further increase in the charge on the Ni_n core and a decreasing electron transfer per C_{60} molecule due to this charging. Thus the IP of the $Ni_n^{\delta+}(C_{60})_m^{\delta-}$ species will probably increase with increasing m following the adsorption of the first C_{60} molecule. If the cluster structure changes with C_{60} adsorption, the pattern of IP changes may become more complex, with cluster size, cluster structure, and C_{60} coverage interacting in a complex way.

The unusual coverage dependence of the $Ni_6(C_{60})_m^+$ ion signal probably results from one or more of the above effects. The observation that Ni_6C_{60} can be ionized by 6.42-eV photons (while Ni_6 cannot) can be explained either by a change in structure of the Ni_6 cluster that lowers its IP, or by there being sufficient electron transfer that ionization can occur directly from C_{60} rather than from the Ni_6 core. At the coverage level of $Ni_6(C_{60})_5$, the total electron transfer to individual C_{60} molecules may be insufficient to allow ionization from the adsorbed C_{60}, and the IP again rises above 6.42 eV. The failure to ionize $Ni_6(C_{60})_2$ and the ease in ionizing $Ni_6(C_{60})_3$ may reflect changes in the Ni_6 structure with increasing coverage that affects both the cluster IP and extent of electron transfer. $Ni_6(C_{60})_4$, as was mentioned above, is not seen with either the ArF or the F_2 laser and likely reflects a rapid adsorbate-induced transition from $Ni_6(C_{60})_3$ to $Ni_6(C_{60})_5$.

In summary, the $Ni_n(C_{60})_m$ species observed in these experiments appear to have solid Ni_n cores with C_{60} molecules adsorbed to specific sites on the surfaces of the clusters, most likely without decomposition. The C_{60}-Ni_n bonds for the initial adsorbed molecules are apparently quite strong and several bonding configurations of the C_{60} molecules to the clusters are likely present. At the high temperatures of the present experiments, relatively free rotation of the C_{60} on the surface of the Ni_n cluster cannot be ruled out. Electron transfer is clearly from the nickel clusters to the adsorbed C_{60} ligands, although the charge actually transferred is expected to be a strong function of coverage and cluster size.

B. Cluster oxides

The presence of an O atom either within the nickel cluster or on its surface frequently alters the uptake of C_{60}. Since its nominal negative charge state O^{2-} is roughly the same as the charge transferred to C_{60} adsorbed on nickel surfaces, an O atom might be expected to replace a C_{60} molecule on the surface of the nickel cluster. For Ni_9-Ni_{15}, the cluster oxides do saturate with one fewer C_{60} molecule than do the pure clusters, suggesting that an O atom is occupying a C_{60} binding site. For Ni_6-Ni_8, the cluster oxides actually saturate with two fewer C_{60} molecules. For Ni_nO with $n \leq 22$, the C_{60} saturation levels are either unchanged or lowered compared with the pure clusters. Abruptly at Ni_{23}, however, the reduction in coverage caused by the O atom is reversed. An oxygen atom on the clusters from Ni_{23-28} actually increases the C_{60} coverage on the cluster [i.e., the presence of the O atom shifts the $Ni_nO(C_{60})_m$ distribution to higher m], although the final saturation level at eight molecules is unchanged. This is the size region where a transition between six to eight adsorbed molecules is occurring, and the presence of an O atom on the cluster appears to facilitate that transition. One possible explanation for this effect is that the O atom withdraws negative charge that would otherwise be on the C_{60} molecules. While this would tend to weaken the directed C_{60}-Ni_n bond, it would also reduce the repulsive forces between the C_{60} molecules in the rather congested cubic configuration (see below). It is this latter effect that may stabilize the cubic

configuration of C_{60} molecules. For clusters larger than 28 atoms, the effect of the O atom on coverage is smaller, sometimes causing a small increase in C_{60} coverage and sometimes causing a decrease.

C. Cluster structures

In this section we will speculate on the possible structures of the nickel clusters that form the core of the $Ni_n(C_{60})_m$ species, taking into account the C_{60} coverage levels observed experimentally at 823 K and a nominal C_{60} pressure of 18 mTorr. We will not discuss every cluster, but limit ourselves to representative examples for each value of *m*. Our purpose here is to demonstrate that in most cases the C_{60} coverages observed at 823 K represent saturation coverages.

It should be realized at the outset that the C_{60}-Ni_n bond strength is much greater than the typical energy differences between the lowest energy isomers of a given Ni_n cluster. For example, Wetzel and DePristo[51] have calculated the lowest energy isomers of Ni_{24-55} and found that for 21 out of the 32 clusters the two lowest energy structures differ by less than 0.1 eV. While smaller clusters often show larger differences, they are generally only fractions of an eV. As a result, we cannot assume that the structures of the metal cores of the $Ni_n(C_{60})_m$ species bear any relationship to the lowest energy bare cluster isomers. The lowered energy due to the C_{60} adsorption may easily cause a rearrangement of the metal core. This is analogous to the surface reconstruction that is often seen when C_{60} is adsorbed on bulk surfaces.[1]

In modeling the $Ni_n(C_{60})_m$ species, we will assume C_{60} is a sphere 10.0 Å in diameter, the spacing observed in bulk C_{60},[39] and the nickel atoms within the Ni_n cluster are spheres separated by the nearest-neighbor distance in the room temperature bulk solid (2.49 Å). Binding is expected to occur between bridge or threefold sites on the metal cluster and the edges or sixfold faces of C_{60}. We do not consider binding between the C_{60} and possible fourfold sites on the metal cluster due to poor symmetry matching. Binding to atop sites on Ni_n is expected to be weak or not occur at all. As discussed below, such binding would often produce coverages in excess of those observed experimentally.

Ni_2, Ni_3. Both Ni_2 and Ni_3 saturate with the adsorption of two C_{60} molecules. In the case of $Ni_2(C_{60})_2$, sideways or end on binding to the dimer is possible. A Ni-C_{60}-Ni-C_{60} linear structure would seem unlikely, since the $Ni_2(C_{60})_3$ species would then be expected, but is not observed. Nikajima *et al.*[15] observed $V_2(C_{60})_3$ at room temperature and attributed it to a linear C_{60}-V-C_{60}-V-C_{60} structure. Nagao *et al.*[16] also observed $Sc_2(C_{60})_3$ and $Ti_2(C_{60})_3$ and proposed similar structures for these species. In view of these results, the absence of $Ni_2(C_{60})_3$ is somewhat surprising, since the Ni_2 bond strength (2.042 eV) (Ref. 52) is actually weaker than the V_2 bond strength (2.753 eV).[53] It is possible that at high temperatures a C_{60} is lost from a linear C_{60}-Ni-C_{60}-Ni-C_{60} species. Kurikawa *et al.*[17] observed $Co_2(C_{60})_4$ and, based on chemical probe experiments, suggested for the structure a Co_2 dimer confined within a distorted tetrahedron of C_{60} molecules. Nagao *et al.*[16] observed $Cr_2(C_{60})_3$ and $Cr_2(C_{60})_4$ and proposed for $Cr_2(C_{60})_3$ a bent structure and for $Cr_2(C_{60})_4$, the same structure proposed for $Co_2(C_{60})_4$.

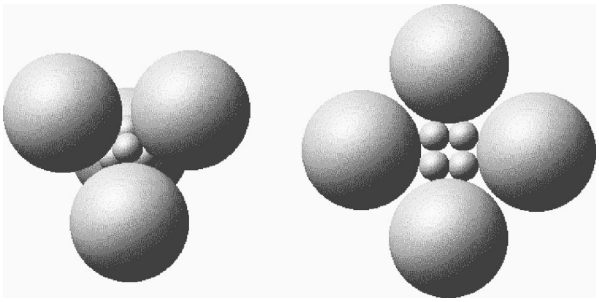

FIG. 13. Two structures for $Ni_4(C_{60})_4$.

In the case of Ni_3, the metal structure is either linear, bent, or triangular if the cluster remains intact. In a triangular configuration, binding two molecules above and below the plane of the triangle to threefold sites competes with binding three molecules in bridging positions in the plane of the triangle (this produces no overlap of the C_{60} molecules). Since only two C_{60} molecules are adsorbed, the bond strength of two threefold sites would have to exceed the bond strength of three bridging C_{60} molecules. Although the evidence from the larger clusters suggests that binding to threefold sites does exceed that for bridge bonding, a 50% increase seems unlikely. Thus, we believe that Ni_3 is probably in a linear or bent configuration in $Ni_3(C_{60})_2$ with the C_{60}'s bound to the end atoms. In the case of V,[15] a $V_3(C_{60})_4$ species was observed and rationalized in terms of a linear chain analogous to the $V_2(C_{60})_3$ species. For $Co_3(C_{60})_4$ (Ref. 17) and $Cr_3(C_{60})_4$,[16] a metal trimer encapsulated within a distorted tetrahedron of C_{60} molecules was proposed.

Ni_4, Ni_5. Both Ni_4 and Ni_5 saturate with the adsorption of four C_{60} molecules. The two most likely structures for an intact nickel core of $Ni_4(C_{60})_4$ are the tetrahedron and the square planar structure shown in Fig. 13. In both cases four C_{60} molecules can be accommodated by the cluster without significant ligand overlap. In the case of the square planar structure, staggering the four C_{60} molecules would result in a larger C_{60}-C_{60} separation. Other, more open structures are possible such as a ring structure suggested for $V_4(C_{60})_4$,[15] but in keeping with the general observation of a central Ni_n core surrounded by adsorbed molecules, we will not consider these structures for Ni_n clusters larger than the trimer.

There are two Ni_5 structures that can support adsorption of four C_{60} molecules, the trigonal bipyramid and the square pyramid. Other structures were considered, including a planar structure, but in all cases some overlap of the C_{60} molecules occurred. The square pyramid can actually support five C_{60} molecules if a C_{60} can be bound to the apex atom as shown in Fig. 14. The failure to observe $Ni_5(C_{60})_5$ suggests that atop binding is relatively weak in comparison to binding to bridge or threefold sites.

Ni_6, Ni_7, Ni_8. Ni_6-Ni_8 all saturate with the adsorption of five C_{60} molecules. The lowest energy isomer for bare Ni_6 is a perfect octahedron.[54] To adsorb five C_{60} molecules on this isomer at least one must be bound to an atop site. This structure is shown in Fig. 15 (left) with the C_{60} that is bound to the atop site (the upper nickel atom) left off. Two C_{60} molecules are bound to bridge sites in the plane of the figure (left and right) and two are bound to threefold sites just below the plane (top and bottom). Six C_{60} molecules can be bound to

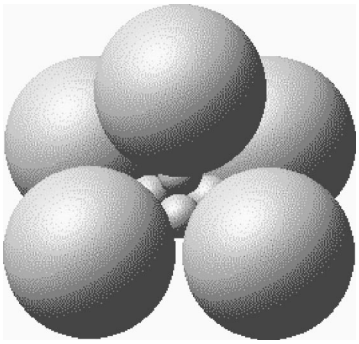

FIG. 14. A possible structure of $Ni_5(C_{60})_5$.

the Ni_6 octahedron if four molecules bind to bridge sites in a plane and two to atop sites above and below the plane. Again, the absence of this structure points to the weakness of atop binding.

A $Ni_6(C_{60})_5$ isomer without atop binding can be obtained with Ni_6 in a hexagonal structure (trigonal prism) as shown in Fig. 15 (right). Although the energy of the bare hexagonal Ni_6 structure may be as much as 0.66 eV higher[55] than the energy of the bare octahedral structure, the absence of atop binding may be sufficient to favor this structure when saturated with C_{60}.

Structures for $Ni_7(C_{60})_5$ and $Ni_8(C_{60})_5$ can be easily derived from the hexagonal structure in Fig. 15 by adding one and two nickel atoms to the unoccupied fourfold sites. $Ni_7(C_{60})_5$ can also be obtained with a capped octahedron for the Ni_7 core, without C_{60} binding to any atop nickel atoms. The capped octahedron, along with the pentagonal bipyramid, are two of the lowest energy Ni_7 isomers.[56]

Ni_9-Ni_{13}. Adding three nickel atoms to three fourfold sites on the Ni_6 trigonal prism [see Fig. 15 (right)] forms the tricapped trigonal prism, which has been determined by Stave and DePristo[54] to be the most stable Ni_9 structure. This readily gives a $Ni_9(C_{60})_5$ species analogous to Fig. 15 (right). Experimentally, however, the clusters between Ni_9 and Ni_{13} first show a preliminary saturation at four C_{60} molecules followed by a structure change leading to adsorption of two additional molecules. $Ni_{13}(C_{60})_6$ appears to be particularly stable, showing no change in coverage with a 200° change in temperature. At the lowest temperature and highest C_{60} pressure, a seventh C_{60} molecule begins to be adsorbed (see Fig. 4). These changes in the adsorption on Ni_{13} are relatively easy to explain. The bare Ni_{13} cluster has been shown to form as an icosahedron.[54] The high symmetry of the icosahedron allows for a number of symmetrical configurations of

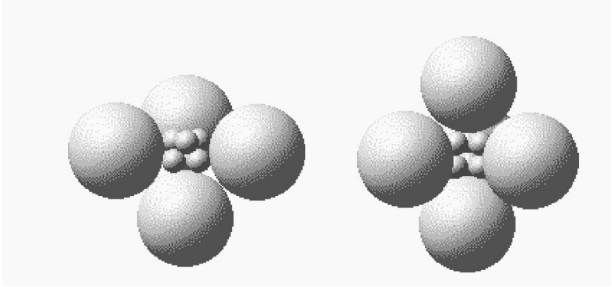

FIG. 15. Two structures for $Ni_6(C_{60})_5$. Left: octahedral (one C_{60} left off). Right: hexagonal.

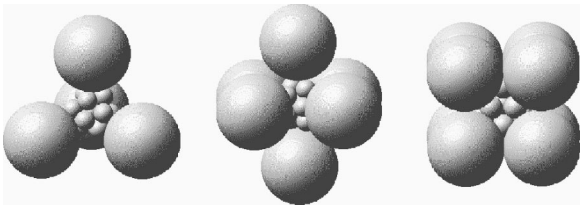

FIG. 16. $Ni_{13}(C_{60})_4$, $Ni_{13}(C_{60})_6$, and $Ni_{13}(C_{60})_8$. Left: tetrahedral; middle: octahedral; right: cubic.

C_{60} molecules on the surface of the cluster. Four molecules can adsorb in a tetrahedral configuration, binding to threefold sites, and six C_{60} molecules can adsorb in an octahedral configuration on bridge sites. These are shown in Fig. 16 (left and middle). Experimentally, the initial change from four to six molecules likely reflects a transition between these two structures. If this is correct, then threefold sites give stronger adsorption of C_{60} than do bridge sites.

Besides the tetrahedral and octahedral configurations, a $Ni_{13}(C_{60})_8$ species can be formed where the eight C_{60} molecules are bound in a cubic configuration, again on threefold sites [Fig. 16 (right)]. In the left and center models, the size of the nickel balls is scaled as indicated earlier. For the cubic geometry these dimensions give some overlap of the C_{60} molecules, so the Ni_{13} cluster is expanded by 20% to give the figure on the right, which shows no overlap. Such an expansion might, for example, arise from the net positive charge on the Ni_{13} cluster as a result of electron transfer to the C_{60} ligands. The adsorption of two additional C_{60} molecules to give Fig. 16 (right) is clearly not complete at the 18 mTorr and 823 K conditions of the experiment, as only the adsorption of a seventh C_{60} molecule is seen. However, this adsorption may involve a rearrangement of the C_{60} ligands to the cubic geometry. The $Ni_{13}(C_{60})_8$ species may never actually form due to excessive repulsive forces between the C_{60} molecules. At higher C_{60} pressures, condensation of C_{60} on top of the first adsorbed layer may occur before the eighth C_{60} molecule can complete the cubic arrangement.

Possible structures of Ni_9 and Ni_{11} can be derived from the $Ni_{13}(C_{60})_6$ structure by removing pairs of adjacent nickel atoms. The structure in Fig. 17 shows the Ni_9 structure after

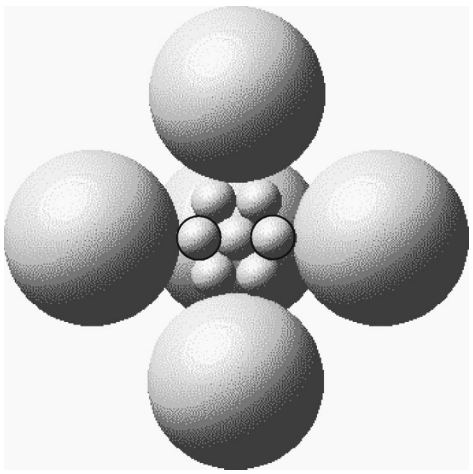

FIG. 17. Possible structure of $Ni_9(C_{60})_6$ (one C_{60} molecule removed).

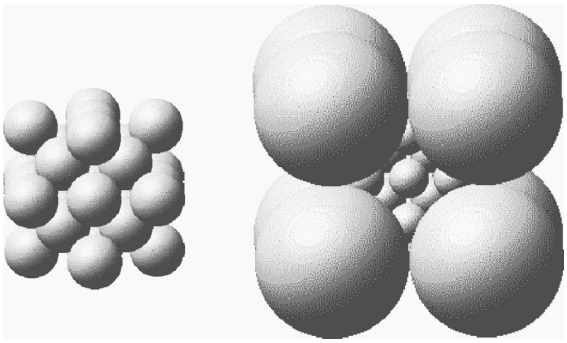

FIG. 18. bcc Ni_{27} and $Ni_{27}(C_{60})_8$.

removing two pairs of nickel atoms from the front and back of the Ni_{13} icosahedron (the front C_{60} has also been removed in order to view the Ni_9 cluster). The resulting Ni_9 isomer has only one fewer Ni-Ni bond than does the most stable Ni_9 isomer (the tricapped trigonal prism) calculated by Stave and DePristo.[54] Bonding between the Ni_9 cluster and C_{60} can occur with two carbon atoms on opposite sides of a sixfold face of C_{60} binding to the two outlined atoms in Fig. 17. No C_{60} overlap occurs. A reasonable Ni_9 structure for the initial saturation level at $Ni_9(C_{60})_4$ is the tricapped octahedron, where all four C_{60} molecules can bind to threefold sites without overlap.

Ni_{14}-Ni_{16}. The special stability of the $Ni_n(C_{60})_6$ saturation level is quite clear from Ni_{13} through at least Ni_{16}. Structure for these species can be obtained from the $Ni_{13}(C_{60})_6$ structure by adding additional nickel atoms to the threefold sites that lie at the center of each triangle of C_{60} molecules [one such site is visible in Fig. 16 (center)]. These atoms do not interfere with the C_{60} bonding to the six bridging sites on the Ni_{13} cluster. Eight nickel atoms, in principle, could be added to give $Ni_{21}(C_{60})_6$; however, only a few are apparently added before a structural rearrangement occurs.

Ni_{24}-Ni_{27}. At 923 and 1023 K there are clear transitions between adsorbing six to adsorbing eight C_{60} molecules. At 923 K, adsorption of eight molecules begins at Ni_{24} and persists until Ni_{30}, and at 1023 K, adsorption of eight molecules begins at Ni_{26} and persists until Ni_{31}. There are no $Ni_n(C_{60})_7$ species in this temperature range. The most compact arrangement of eight C_{60} molecules that leaves room in the center for the Ni_n cluster is a cube. In this size range a reasonable candidate for the Ni_n structure is the bcc cube shown in Fig. 18 (left) for 27 atoms. The same cluster covered with eight C_{60} molecules is shown in Fig. 18 (right). With the eight C_{60} molecules located at the eight corners of the cubic structure, there is no overlap. A possible bonding configuration is shown in Fig. 19, where three of the four nickel atoms at the corners of the cube bind in bridging positions to edge sites on C_{60}. The smaller clusters that occur with saturation at eight [beginning at $Ni_{24}(C_{60})_8$] can be formed by removing atoms from the centers of the faces of the cubic structure.

The next closed shell of C_{60} molecules occurs at 12. Twelve C_{60} molecules can be adsorbed on Ni_{55} in its most stable, icosahedral geometry,[46,52] but only if they are bound to the 12 apex atoms. By removing the 12 apex atoms a 43-atom cluster in the form of a pentagonal dodecahedron results. Twelve C_{60} molecules can be placed on the 12 pentagons of this cluster with the ligands just touching. However, saturation of these two clusters occurs with the adsorption of only ten C_{60} molecules. In the case of Ni_{55}, the weakness of atop binding is probably the limitation. In the case of Ni_{43}, the structure obtained by removing the 12 apex atoms from the 55-atom icosahedron is likely too unstable.[57]

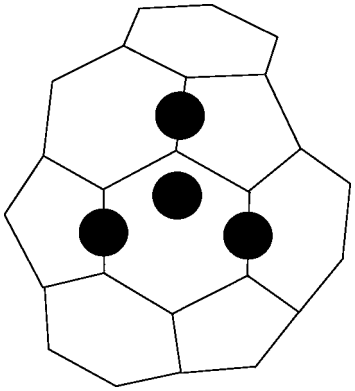

FIG. 19. Possible bonding configuration.

In the absence of a highly symmetrical configuration of acceptable binding sites, the saturation coverage may be reduced considerably from the hypothetical closed-packed limit. If the C_{60} binding is restricted to bridge and threefold sites on the 55-atom icosahedron, the highest coverage that we have found is $Ni_{55}(C_{60})_{10}$, in agreement with the experimental result. In Fig. 20, we show one such configuration of ten binding sites. In Fig. 20 the faces of the icosahedron have been stretched out to view the cluster. The small figure to the lower right corresponds to a mirror image of the five faces on the back side of the cluster. The white and gray circles represent the atoms on the surface of the 55-atom icosahedron (the gray circles are the 12 apex atoms). The outer ten circles on both figures correspond to the same atoms. The black circles represent threefold binding sites for C_{60} and the black rectangles represent bridge sites. There is no overlap of the adsorbed C_{60} molecules. Other arrangements of the ten sites are also possible, but we have not found more than ten such sites.

The fcc cuboctahderon also forms a closed shell at 55 atoms; however, we have been unable to place ten C_{60} molecules on this cluster without C_{60} binding to at least two atop sites.

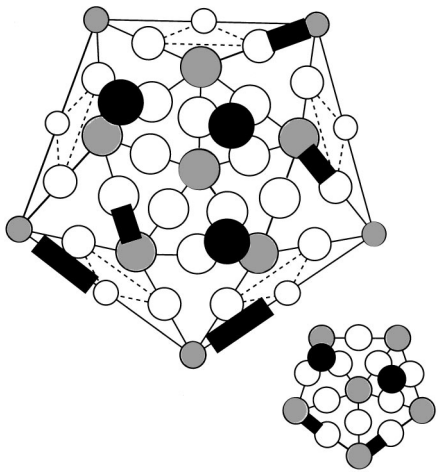

FIG. 20. C_{60} binding on the 55-atom icosahedron.

A similar analysis of the 71-atom capped icosahedron shows that 12 C_{60} molecules can readily be placed on this cluster in bridge and threefold sites, in agreement with the observed saturation level of $Ni_{71}(C_{60})_{12}$, and we have not found configurations with more than 12 molecules.

It might be noted that 32 C_{60} molecules can be placed on the Ni_{309} icosahedral cluster (four shells surrounding a central atom) in a closed-packed arrangement. Twenty of the molecules can be placed in the centers of the 20 faces of the icosahedron on threefold sites, forming a pentagonal dodecahedron of C_{60} molecules, while the remaining 12 molecules would sit atop the 12 apex nickel atoms. Due to the expected stability of the Ni_{309} cluster[58] and the apparent preference for binding to threefold sites, the $Ni_{309}(C_{60})_{20}$ species (without the molecules on the apex sites) might be expected to be especially stable. The present experiments did not investigate clusters in this size range.

From the above discussion, we draw three conclusions: (1) C_{60} binding appears to be weaker to atop sites than to bridge and threefold sites on the nickel cluster. If this were not true, saturation levels would frequently be higher than those observed experimentally; (2) the coverages that are obtained with C_{60} bound to bridge and threefold sites on reasonable Ni_n structures are in excellent agreement with the experimentally determined saturation levels. We believe that at a temperature of 823 K and the nominal C_{60} pressure of 18 mTorr, the clusters, in most cases, have saturated coverages of C_{60}; and (3) the pattern of jumps in coverage $4\rightarrow6\rightarrow8$ and probably the $10\rightarrow12$ jump reflect changes in the configuration of the C_{60} ligands as a result of the increasing size of the central Ni_n cluster.

V. SUMMARY

The adsorption of C_{60} on nickel clusters has been studied from Ni_2 through Ni_{72} over a temperature range from 823 to 1073 K. At the lowest temperature, the adsorption leads to saturation coverages of C_{60} on essentially spherical nickel clusters. At the highest temperature, equilibrium adsorption is apparent and the coverage decreases. There is no evidence for C_{60} decomposition. The first C_{60} molecule that binds to the nickel clusters appears to have a binding energy in excess of 2.06 eV. The C_{60}-Ni_n bond strength appears to increase with increasing metal nuclearity of the binding site, with binding to atop sites being particularly weak. The number of C_{60} molecules adsorbed on the clusters at saturation appears to be governed largely by the number of C_{60} spheres that can be packed around the small nickel clusters. The packing appears to change from tetrahedral to octahedral to cubic and finally to a less symmetric packing at larger cluster sizes.

ACKNOWLEDGMENTS

We would like to thank Dr. Geoff Koretsky and Professor George Nieman for assistance with the experiments and many useful discussions. This work was supported by the U.S. Department of Energy, Office of Basic Energy Sciences, Division of Chemical Sciences, under Contract No. W-31-109-Eng-38.

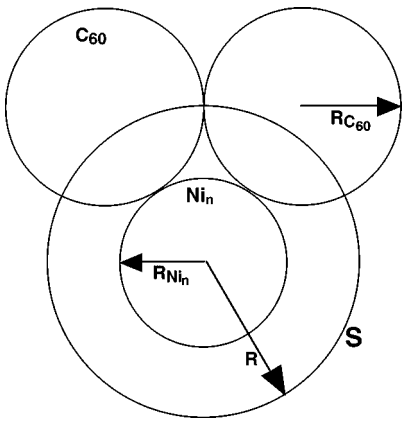

FIG. 21. Schematic of two C_{60} molecules bound to a nickel cluster.

APPENDIX

When covering a spherical nickel cluster with a group of C_{60} spheres, it is necessary to calculate the effective area of the nickel surface occupied by a C_{60} sphere. This is illustrated in Fig. 21. The ''surface area'' of the Ni_n cluster occupied by a single C_{60} molecule can be best referenced to a spherical surface S that passes through the contact points of the adsorbed C_{60} molecules (at a distance R from the center of the cluster). The area $A_{C_{60}}$ of the surface S occupied by a single C_{60} molecule is that portion of the surface S that intersects one of the C_{60} spheres. With $\gamma = R_{Ni_n}/R_{C_{60}}$, $R^2 = R_{C_{60}}^2(2\gamma+\gamma^2)$ and the area $A_{C_{60}}$ is given by

$$A_{C_{60}} = 2\pi R^2\left(1-\frac{\sqrt{2\gamma+\gamma^2}}{1+\gamma}\right).$$

As $\gamma\rightarrow\infty$, $A\rightarrow\pi R_{C_{60}}^2$, as it should for a flat surface. $4\pi R^2$ is the effective area of the metal surface that the C_{60} spheres sit on. The fractional area occupied by spheres close packed on a flat surface is $\pi/(2\sqrt{3}) = 0.907$. Close packing spheres on another sphere, however, is generally not possible, resulting in a packing fraction that is usually less than 0.907. The packing fraction is related to the quantity α in Fig. 12 by

$$\alpha R^2 = \text{packing fraction}\times\left(\frac{4\pi R^2}{A_{C_{60}}}\right).$$

The packing fraction is $\sim$0.7 for the largest clusters studied here ($\alpha = 0.14$ in Fig. 12).[59]

[1] P. Rudolf in *Fullerenes and Fullerene Nanostructures*, edited by H. Kuzmany, J. Fink, M. Mehring, and S. Roth (World Scientific, New Jersey, 1996).
[2] F. Tast, N. Malinowski, S. Frank, M. Heinebrodt, I. M. L. Billas, and T. P. Martin, Z. Phys. D **40**, 351 (1997); U. Zimmermann, N. Malinowski, A. Burkhardt, and T. P. Martin, Carbon **33**, 995 (1995).
[3] L. Ruan and D. M. Chen, Surf. Sci. **393**, L113 (1997).
[4] T. R. Ohno, Y. Chen, S. E. Harvey, G. H. Kroll, P. J. Benning, J. H. Weaver, L. P. F. Chibante, and R. E. Smalley, Phys. Rev. B **47**, 2389 (1993).
[5] M. Stetzer, P. Heiney, J. Fischer, and A. McGhie, Phys. Rev. B **55**, 127 (1997).
[6] M. Foltin, M. Lezius, P. Scheier, and T. D. Märk, J. Chem. Phys. **98**, 9624 (1993).
[7] P. Wurz and K. R. Lykke, J. Phys. Chem. **96**, 10 129 (1992).
[8] E. E. B. Campbell, G. Ulmer, H. G. Bussmann, and I. V. Hertel, Chem. Phys. Lett. **175**, 505 (1990).
[9] K. Hansen and O. Echt, Phys. Rev. Lett. **78**, 2337 (1997).
[10] E. E. B. Campbell, G. Ulmer, and I. V. Hertel, Phys. Rev. Lett. **67**, 1986 (1991).
[11] F. Tast, N. Malinowski, S. Frank, M. Heinebrodt, I. M. L. Billas, and T. P. Martin, Phys. Rev. Lett. **77**, 3529 (1996).
[12] W. Branz, I. M. L. Billas, N. Malinowski, F. Tast, M. Heinebrodt, and T. P. Martin, J. Chem. Phys. **109**, 3425 (1998).
[13] C. Cepek, A. Goldoni, and S. Modesti, Phys. Rev. B **53**, 7466 (1996).
[14] A. J. Maxwell, P. A. Brühwiler, S. Andersson, N. Mårtensson, and P. Rudolf, Chem. Phys. Lett. **247**, 257 (1995).
[15] A. Nakajima, S. Nagao, H. Takeda, T. Kurikawa, and K. Kaya, J. Chem. Phys. **107**, 6491 (1997).
[16] S. Nagao, T. Kurikawa, K. Miyajima, A. Nakajima, and K. Kaya, J. Phys. Chem. **102**, 4495 (1998).
[17] T. Kurikawa, S. Nagao, K. Miyajima, A. Nakajima, and K. Kaya, J. Phys. Chem. **102**, 1743 (1998).
[18] Ch. Kusch, B. Winter, R. Mitzner, A. Gomes Silva, E. E. B. Campbell, and I. V. Hertel, Chem. Phys. Lett. **275**, 469 (1997).
[19] S. C. Richtsmeier, E. K. Parks, K. Liu, L. G. Pobo, and S. J. Riley, J. Chem. Phys. **82**, 3659 (1985).
[20] P. S. Bechthold, E. K. Parks, B. H. Weiller, L. G. Pobo, and S. J. Riley, Z. Phys. Chem., Neue Folge **169**, 101 (1990).
[21] As an example, with the FTR at 1073 K, a $Ni_{13}(C_{60})_6$ cluster emerges from the nozzle expansion with roughly 70 eV of translational energy along the cluster beam axis. This energy was determined by modeling the mass spectrometer with the program MACSIMION and determining the energy from the experimentally determined deflection plate voltage settings for $Ni_{13}(C_{60})_6^+$.
[22] E. K. Parks, L. Zhu, J. Ho, and S. J. Riley, J. Chem. Phys. **100**, 7206 (1994).
[23] Cluster cooling in the nozzle expansion prevents C_{60} desorption between the nozzle and the time-of-flight mass spectrometer.
[24] E. K. Parks, G. C. Nieman, K. P. Kerns, and S. J. Riley, J. Chem. Phys. **107**, 1861 (1997).
[25] The value of 18 mTorr is best considered an upper limit. The average He flow velocity in the FTR was used in determining the C_{60} pressure. Since the C_{60} distribution across the diameter of the FTR is to some extent concentrated in the center (where the He flow velocity is twice the average), the C_{60} flow velocity is somewhere between the average He flow velocity and twice that velocity. As a result, the C_{60} pressure is likely somewhat lower than 18 mTorr but certainly greater than 10 mTorr. At the cup temperature that produces the nominal 18 mTorr C_{60} vapor pressure, the static vapor pressure above solid C_{60} is ~1.1 Torr [extrapolated from the data of J. Abrefah, D. R. Olander, M. Balooch, and W. J. Siekhaus, Appl. Phys. Lett. **60**, 1313 (1992)]. The nominal vapor pressure in the FTR is lower due to the low rate of diffusion of C_{60} out of the cup into the helium carrier gas. To monitor the C_{60} pressure in the present experiments, the C_{60}^+ ion signal in the mass spectrum was followed over the lifetime of the sample in the cup.
[26] Clusters with the same mass but different numbers of adsorbed C_{60} molecules acquire different energies in the nozzle expansion, which results in slightly different trajectories through the mass spectrometer and thus slightly different flight times.
[27] E. K. Parks, K. P. Kerns, G. M. Koretsky, G. C. Nieman, and S. J.Riley (unpublished).
[28] MER stands for Materials & Electrochemical Research Corporation (Tucson, AZ).
[29] Frankfurt, Germany.
[30] This peak is actually two peaks separated by 8 amu.
[31] M. B. Knickelbein, S. H. Yang, and S. J. Riley, J. Chem. Phys. **93**, 94 (1990); E. K. Parks, T. D. Klots, and S. J. Riley, *ibid.* **92**, 3813 (1990).
[32] Ni^+ was also observed, but is thought to arise mainly from fragmentation processes.
[33] While Ni^+ and $Ni(C_{60})_2^+$ are also observed, they are thought to arise, at least in part, from fragmentation processes.
[34] In a process dominated by adsorption kinetics (i.e., no desorption of the adsorbed molecules), as saturation at $Ni_n(C_{60})_p$ is approached the accumulation of the $Ni_n(C_{60})_m$ product species can cause a bimodal distribution to form of the p-2, p-1, p species; i.e., the intensity of the p-1 species can become smaller than that of the p-2 and p species. This cannot occur under equilibrium conditions as long as the adsorption bond strength decreases continuously with increasing coverage.
[35] Unpublished results from this laboratory.
[36] P. J. Benning, D. M. Poirier, T. R. Chen, M. B. Jost, F. Stepniak, G. H. Kroll, J. H. Weaver, J. Fure, and R. E. Smalley, Phys. Rev. B **45**, 6899 (1992).
[37] H.-B. Bürgi, R. Restori, and D. Schwarzenbach, Acta Crystallogr., Sect. B: Struct. Sci. **B49**, 832 (1993).
[38] In the structureless packing model one equates the volume of the cluster to the number of atoms in the cluster times the atomic volume using the bulk density.
[39] J. Bohr, D. Gibbs, S. K. Sinha, W. Krätschmer, G. van Tendeloo, E. Larson, H. Egsgaard, and L. E. Berman, Europhys. Lett. **17**, 327 (1992).
[40] A preexponential factor of 4.3×10^{12} monolayers/s has been obtained for zero-order desorption of C_{60} multilayers; see A. V. Hamza and M. Balooch, Chem. Phys. Lett. **198**, 603 (1992).
[41] T. Quest, R. Bellmann, B. Winter, J. Gatzke, and I. V. Hertel, J. Appl. Phys. **83**, 1642 (1998).
[42] M. R. C. Hunt, S. Modesti, P. Rudolf, and R. E. Palmer, Phys. Rev. B **51**, 10 039 (1995).
[43] E. K. Parks, G. C. Nieman, K. P. Kerns, and S. J. Riley, J. Chem. Phys. **108**, 3731 (1998).
[44] F. Ercolessi, W. Andreoni, and E. Tosatti, Phys. Rev. Lett. **66**, 911 (1991).
[45] E. K. Parks, L. Zhu, J. Ho, and S. J. Riley, J. Chem. Phys. **102**, 7377 (1995).
[46] E. K. Parks, B. J. Winter, T. D. Klots, and S. J. Riley, J. Chem. Phys. **94**, 1882 (1991).
[47] R. Fasel, P. Aebi, R. G. Agostino, D. Naumović, J. Osterwalder,

A. Santaniello, and L. Schlapbach, Phys. Rev. Lett. **76**, 4733 (1996).

[48] E. I. Altman and R. J. Colton, Surf. Sci. **279**, 49 (1992); Phys. Rev. B **48**, 18 244 (1993).

[49] S. Modesti, S. Cerasari, and P. Rudolf, Phys. Rev. Lett. **71**, 2469 (1993); P. J. Benning, F. Stepniak, and J. H. Weaver, Phys. Rev. B **48**, 9086 (1993); L. Q. Jiang and B. E. Koel, Chem. Phys. Lett. **223**, 69 (1994); Phys. Rev. Lett. **72**, 140 (1994); A. J. Maxwell, P. A. Brühwiler, S. Andersson, N. Mårtensson, and P. Rudolf, Chem. Phys. Lett. **247**, 257 (1995).

[50] These effects have been observed for adsorption of hydrogen and carbon monoxide on nickel clusters. The opposite result of increased ionization efficiency and decreased IP resulting from electron donation to the metal from the ligand have been observed for ammonia adsorption [see E. K. Parks, T. D. Klots, and S. J. Riley, J. Chem. Phys. **92**, 3813 (1990); M. Knickelbein and W. J. C. Menezes, *ibid.* **94**, 4111 (1991)]. Nitrogen adsorption, which transfers little charge in either direction, has little effect on the ionization efficiency or IP.

[51] T. L. Wetzel and A. E. DePristo, J. Chem. Phys. **105**, 572 (1996).

[52] J. C. Pinegar, J. D. Langenberg, C. A. Arrington, E. M. Spain, and M. D. Morse, J. Chem. Phys. **102**, 666 (1995).

[53] E. M. Spain, J. M. Behm, and M. D. Morse, J. Chem. Phys. **96**, 2511 (1992).

[54] M. S. Stave and A. E. DePristo, J. Chem. Phys. **97**, 3386 (1992).

[55] E. Curotto, A. Matro, D. L. Freeman, and J. D. Doll, J. Chem. Phys. **108**, 729 (1998).

[56] N. Desmarais, C. Jamorski, F. A. Reuse, and S. N. Khanna, Chem. Phys. Lett. **294**, 480 (1998).

[57] Removing the 12 apex atoms from the 55-atom icosahedron breaks eight more Ni-Ni bonds than does removing 12 contiguous nickel surface atoms. The binding of two additional C_{60} molecules apparently does not compensate for this loss in Ni-Ni bonding.

[58] M. Pellarin, B. Baguenard, J. L. Vialle, J. Lermé, M. Broyer, J. Miller, and A. Perz, Chem. Phys. Lett. **217**, 349 (1994).

[59] The cluster radius and thus the quantity $A_{C_{60}}$ determined by the structureless packing model increase in validity as the cluster size increases.